

Estimating the Properties of Naturally Fractured Reservoirs Using Rate Transient Decline Curve Analysis

Amin Daryasafar^{1*}, Mohammad Joukar^{2*}, Mohammad Fathinasab³,
Giovanni Da Prat⁴, Riyaz Kharrat¹

1. Petroleum Department, Petroleum University of Technology, Ahwaz 6198144471, Iran

2. Department of Petroleum Engineering, National Iranian South Oilfields Company (NISOC), Ahwaz 6163756686, Iran

3. Department of Chemical and Petroleum Engineering, Sharif University of Technology, Tehran 11365-11155, Iran

4. Da Prat & Associates (Consulting Company), Buenos Aires C1420, Argentina

¹Amin Daryasafar: <http://orcid.org/0000-0002-5167-6014>; ²Mohammad Joukar: <http://orcid.org/0000-0002-8535-5737>

ABSTRACT: Transient rate decline curve analysis for constant pressure production is presented in this paper for a naturally fractured reservoir. This approach is based on exponential and constant bottom-hole pressure solution. Based on this method, when \ln (flow rate) is plotted versus time, two straight lines are obtained which can be used for estimating different parameters of a naturally fractured reservoir. Parameters such as storage capacity ratio (ω), reservoir drainage area (A), reservoir shape factor (C_A), fracture permeability (k_f), interporosity flow parameter (λ) and the other parameters can be determined by this approach. The equations are based on a model originally presented by Warren and Root and extended by Da Prat et al. and Mavor and Cinco-Ley. The proposed method has been developed to be used for naturally fractured reservoirs with different geometries. This method does not involve the use of any chart and by using the pseudo steady state flow regime, the influence of wellbore storage on the value of the parameters obtained from this technique is negligible. In this technique, all the parameters can be obtained directly while in conventional approaches like type curve matching method, parameters such as ω and λ should be obtained by other methods like build-up test analysis and this is one of the most important advantages of this method that could save time during reservoir analyses. Different simulated and field examples were used for testing the proposed technique. Comparison between the obtained results by this approach and the results of type curve matching method shows a high performance of decline curves in well testing.

KEY WORDS: naturally fractured reservoirs, rate transient decline curve analysis, well testing, pseudo-steady state condition, bounded reservoirs.

0 INTRODUCTION

Naturally fractured reservoirs are porous media which host more than 50% of the world hydrocarbon reserves (Gutmanis, 2009). These porous media consist of matrix blocks and fractures and because of this, mechanism of fluid flow through these reservoirs is not still well understood (Gang and Kelkar, 2006). Most of the fluid is stored in the matrix blocks but these blocks have low permeability. In comparison, the fractures have high permeability but they do not store much. Most of the reservoir fluid flows from the matrix blocks into the wellbore through the permeable fractures. The matrix-fracture fluid transport capacity governs the producing capacity of a naturally fractured reservoir. This is called interporosity flow (Abbasi et al., 2016).

The behavior of naturally fractured reservoirs (NFR) at

pseudo-steady state is similar to that of a homogeneous reservoir (Igbokoyi and Tiab, 2006). However, since there is a double porosity nature, the behavior is quite different. Also, taking matrix flow into account is very important for estimating different parameters of a naturally fractured reservoir. Therefore, a powerful method for determining naturally fractured reservoir properties is needed.

In the dual porosity, two major parts are considered for a reservoir: matrix and fractures. Based on Warren and Root (1963), naturally fractured reservoirs are visualized as a set of stacked cubes. In this method, the matrix acts as a source which contains most of the fluid and fractures are the main flow paths. Transfer functions define the fluid transfer between the matrix and the fractures. Several researchers have introduced a range of different transfer functions for simulating the fluid flow in large scales (Bourbiaux et al., 1999; Gilman, 1986; Pruess, 1985; Duguid and Lee, 1977). Landereau et al. (2001) proposed a new approach for simulating flow in fractured media. This technique has been created to separate the fracture systems and the matrix in order to simplify the complexity in the matrix-fracture behavior. Noetinger and Estebenet (2000) presented a new method which is an alternative to the classical double porosity models for upscaling and modeling flow in fractured masses. This technique is called

*Corresponding author: amindaryasafar@yahoo.com;

mohammad.joukar@gmail.com

© China University of Geosciences and Springer-Verlag GmbH Germany 2017

Manuscript received April 16, 2017.

Manuscript accepted June 15, 2017.

continuous time random walk (CTRW).

One of the applications of classical double porosity methods is the analysis of pressure transient data from fractured reservoirs. This approach was presented by Warren and Root (1963). In this method, the fluid flow from the matrix to the fracture is pseudo-steady state. De Swaan (1990) proposed a mathematical model for matrix transient flow but the results were never matched for well test analysis. For matrix transient flow and double porosity well test analysis, slab model has been mostly used rather than other models. Most of the methods that have been presented for estimating the properties of naturally fractured reservoirs are based on pressure transient. These methods are classified into two main categories: Tiab direct synthesis (TDS) and conventional techniques for instances Horner plot and type curve matching.

Tiab direct synthesis (Tiab, 1995, 1994) is a technique based on interpreting pressure transient data for estimating naturally fractured reservoirs properties. This method utilizes the slopes and intersection points of different straight lines from a log-log plot of pressure and pressure derivative data points. This method has some advantages such as get accurate results with or without observation of all reservoir flow regimes, results are obtained from exact and analytical equations and also, possibility of independent verification from a third unique point. However, these methods, including conventional approaches, are time-consuming methods and different plots of pressure and pressure derivatives with software analyses are needed. Therefore, it is crucial to propose a simple method with acceptable accuracy that can estimate all the parameters of a naturally fractured reservoir.

In this paper, rate transient decline curve analysis has been developed for closed naturally fractured reservoirs. In this technique, the plot of rate versus time is needed, so it requires production at constant pressure and pseudo-steady state flow condition. In order to obtain this procedure, an equation for fracture depletion that is given by Mavor and Cinco-Ley (1979) and an equation for matrix+fracture depletion (total system depletion) which is given by Da Prat et al. (1981) were used. These equations are based on Warren and Root model and they are for pseudo-steady state condition. When natural logarithm is taken from two sides of fracture and fracture+matrix depletion equations, two straight lines are obtained. Then, the slopes and intercepts of these lines are used to determine different properties and characteristics of a naturally fractured reservoir. The main limitation of this technique is that it requires a short build-up test so that the skin factor could be estimated.

1 MODEL DEVELOPMENT

The main objective of this study is to find solutions for bounded and closed naturally fractured reservoirs. A bounded naturally fractured reservoir in rate transient test shows a rapid decline at first, then an almost constant flow rate for a long time, after which a final rate decline takes place (Da Prat et al., 1981). In other words, the fracture depletion dominates for shorter times while the fracture+matrix depletion (total system depletion) dominates for longer times. Each period can be characterized by a specific equation. Based on this fact, a method can be proposed for determining different properties of a naturally fractured reservoir.

The fundamental partial differential equations for cylindrical, naturally fractured reservoirs are (Da Prat et al., 1981)

$$\frac{\partial^2 p_{fD}}{\partial r_D^2} + \frac{1}{r_D} \frac{\partial p_{fD}}{\partial r_D} = (1-\omega) \frac{\partial p_{mD}}{\partial t_D} + \omega \frac{\partial p_{fD}}{\partial t_D} \quad (1)$$

and

$$(1-\omega) \frac{\partial p_{mD}}{\partial t_D} = \lambda(p_{fD} - p_{mD}) \quad (2)$$

For matrix and fracture, the dimensionless flow rate, q_D and dimensionless pressure, p_D are as follows

$$p_D = \frac{k_f h (p_i - p_{wf})}{141.2 q \mu B} \quad (3)$$

$$q_D = 141.2 \frac{q \mu B}{k_f h (p_i - p_{wf})} \quad (4)$$

Da Prat et al. (1981) solved Eq. (1) for the general pseudo-steady state and finite system solution as follow

$$\begin{aligned} \bar{q}_D(s) = & \frac{\sqrt{sf(s)}}{s} \times \\ & \frac{\left[I_1(\sqrt{sf(s)} r_{eD}) k_1(\sqrt{sf(s)}) - k_1(\sqrt{sf(s)} r_{eD}) I_1(\sqrt{sf(s)}) \right]}{\left[k_1(\sqrt{sf(s)} r_{eD}) I_0(\sqrt{sf(s)}) + I_1(\sqrt{sf(s)} r_{eD}) k_0(\sqrt{sf(s)}) \right]} \end{aligned} \quad (5)$$

where

$$f(s) = \frac{\omega(1-\omega)s + \lambda}{(1-\omega)s + \lambda} \quad (6)$$

It must be noticed that this solution is for radial flow. In order to find a general solution for reservoirs with different geometries, the solution must be transformed using shape factor (C_A). Inverse Laplace transformation should be applied in order to find the solution in time. Different methods can be used for this purpose (Abramowitz and Stegun, 1972; Stehfest, 1970).

As mentioned before, two decline periods are shown for a closed naturally fractured reservoir in rate transient test: a first rapid decline which belongs to the fracture depletion and a final decline that belongs to the total system depletion. Mavor and Cinco-Ley (1979) presented a solution for fracture depletion

$$p_{Df} = \frac{2\pi t_{DA}}{\omega} + \frac{1}{2} \ln \left(\frac{2.2458A}{C_A r_w^2} \right) \quad (7)$$

where

$$t_{DA} = \frac{t_D}{A} r_w^2$$

Applying Laplace transform yields

$$\bar{p}_{Df} = \frac{2\pi}{\omega s^2} + \frac{1}{2s} \ln \left(\frac{2.2458A}{C_A r_w^2} \right) \quad (8)$$

This expression is valid for $t_{DA}/\omega \geq 0.1$.

Van Everdingen and Hurst (1949) showed that constant pressure and constant rate problems could be related to each other in Laplace space by

$$\bar{p}_D \bar{q}_D = \frac{1}{s^2} \quad (9)$$

From Eqs. (8) and (9) and then applying the inverse Laplace transforms

$$q_{Df} = \frac{2}{\ln\left(\frac{2.2458A}{C_A r_w^2}\right)} \text{Exp}\left[\frac{-4\pi r_w^2 t_D}{A\omega \ln\left(\frac{2.2458A}{C_A r_w^2}\right)}\right] \quad (10)$$

This equation is used for first rapid flow depletion, fracture depletion, at pseudo-steady state flow and constant bottom-hole pressure condition. If natural logarithm is taken from both sides of this equation, a straight line could be obtained with slope m_{Df} and an intercept b_{Df} as follow

$$m_{Df} = \frac{-4\pi r_w^2}{A\omega \ln\left(\frac{2.2458A}{C_A r_w^2}\right)} \quad (11)$$

$$b_{Df} = \frac{2}{\ln\left(\frac{2.2458A}{C_A r_w^2}\right)} \quad (12)$$

Da Prat et al. (1981) presented a solution for fracture+ matrix depletion at pseudo-steady state and constant bottom-hole pressure condition as follow

$$q_{Dm} = \frac{\left(\frac{A}{r_w^2} - \pi\right)\lambda}{2\pi} \exp\left(\frac{-\lambda t_D}{(1-\omega)}\right) \quad (13)$$

If natural logarithm is taken from both sides of Eq. (13), a straight line could be obtained with slope m_{Dm} and an intercept b_{Dm} as follow

$$m_{Dm} = \frac{-\lambda}{(1-\omega)} \quad (14)$$

$$b_{Dm} = \frac{\left(\frac{A}{r_w^2} - \pi\right)\lambda}{2\pi} \quad (15)$$

Dimensionless slope and intercept parameters should be defined in order to simplify the relations and also relate the parameters together. For this purpose, the following dimensionless variables are defined for estimating naturally fractured reservoir parameters (these parameters are evaluated in Appendix A).

$$m_D = 873.3m \frac{[(\phi c_t)_f + (\phi c_t)_m] \mu r_w^2}{k_f} \quad (16)$$

$$b_D = 141.2 \frac{b\mu B}{k_f h(p_i - p_{wf})} \quad (17)$$

$$t_D = 2.637 \times 10^{-4} \frac{k_f t}{[(\phi c_t)_f + (\phi c_t)_m] \mu r_w^2} \quad (18)$$

Now from Eqs. (11) and (12)

$$\omega = \frac{-2\pi r_w^2 b_{Df}}{A m_{Df}} \quad (19)$$

From Eqs. (14) and (15) and according to this assumption that $A / (\pi r_w^2) - 1 \approx A / (\pi r_w^2)$ then

$$\omega = 1 + \frac{2\pi r_w^2 b_{Dm}}{A m_{Dm}} \quad (20)$$

From Eqs. (19) and (20)

$$A = -2\pi r_w^2 \left(\frac{b_{Df}}{m_{Df}} + \frac{b_{Dm}}{m_{Dm}}\right) \quad (21)$$

These slopes and intercepts are used for estimating different parameters of a naturally fractured reservoir. It must be noticed that the unknown parameters are more than equations; therefore, an excess equation is needed. For solving this problem an equation which is based on Warren and Root pseudo-steady state flow (Warren and Root, 1963), Eq. (37), is presented. This equation will be discussed in Section 1.3.

1.1 Storage Capacity Ratio Estimation

From Eq. (20) and Eq. (21) and since $(b_{Df}/m_{Df})/(b_{Dm}/m_{Dm}) = (b_f/m_f)/(b_m/m_m)$, then

$$\omega = \frac{(b_f / m_f)}{(b_f / m_f + b_m / m_m)} \quad (22)$$

From the above equation storage capacity ratio can be determined. The dimensionless parameter (ω) defines the storativity of the fractures as a ratio to that of the total reservoir. Mathematically, it is given by

$$\omega = \frac{(\phi c_t)_f}{(\phi c_t)_f + (\phi c_t)_m} \quad (23)$$

By estimating storage capacity ratio, fracture storage capacity can be determined as follow

$$(\phi c_t)_f = (\phi c_t)_m \left(\frac{\omega}{1-\omega}\right) \quad (24)$$

According to the above: $(\phi c_t)_t = (\phi c_t)_m + (\phi c_t)_f$ which is total storage capacity.

1.2 Reservoir Drainage Area Estimation

Using Eqs. (16) and (17) for matrixes

$$\frac{b_{Dm}}{m_{Dm}} = 0.016 \frac{b_m B}{m_m} \times \frac{1}{[(\phi c_t)_m + (\phi c_t)_f] h r_w^2 (p_i - p_{wf})} \quad (25)$$

Using Eqs. (16) and (17) for fractures

$$\frac{b_{Df}}{m_{Df}} = 0.016 \frac{b_f B}{m_f} \times \frac{1}{[(\phi c_t)_m + (\phi c_t)_f] h r_w^2 (p_i - p_{wf})} \quad (26)$$

From Eqs. (21), (25), and (26) we can estimate reservoir drainage area as accurately as possible as follows

$$A = -0.1005 \frac{B}{h(p_i - p_{wf})} \left[\frac{b_f}{m_f} + \frac{b_m}{m_m}\right] \times \frac{1}{(\phi c_t)_m + (\phi c_t)_f} \quad (27)$$

1.3 Reservoir Shape Factor Estimation

Since the unknowns of this method are more than equations we have, in this section a method is suggested to calculate reservoir shape factor, approximately. We know that for $t_D > [\omega(1-\omega)]/\lambda$, the equation proposed by Warren and Root (1963) for pseudo-steady state flow is as follows

$$p_{wD} = \frac{2\pi t_D r_w^2}{A} + \frac{1}{2} \ln \left(\frac{2.2458A}{C_A r_w^2} \right) + \frac{2\pi(1-\omega)^2 r_w^2}{\lambda A} \quad (28)$$

and

$$p_D = \frac{k_f h}{141.2q\mu B} (p_i - p_{wf}) \quad (29)$$

Recall that C_A for a circular reservoir is 31.62, and then the term $[2\pi(1-\omega)^2 r_w^2] / \lambda A$ in Eq. (28) can be replaced by $[0.1987C_A(1-\omega)^2 r_w^2] / \lambda A$.

Combining Eq. (12), Eq. (15), Eq. (17), Eq. (18), Eq. (28) and Eq. (29), the following equation can be solved for C_A

$$\begin{aligned} & \frac{h(p_i - p_{wf})}{141.2q\mu B} \\ &= \frac{2.637 \times 10^{-4} \times 2\pi t}{A\mu(\phi c)_i} \\ &+ \frac{h(p_i - p_{wf})}{141.2b_f\mu B} \\ &+ \frac{0.1987C_A(1-\omega)^2 h(p_i - p_{wf})}{887.186b_m\mu B} \end{aligned} \quad (30)$$

The above equation can be simplified by substituting Eq. (27) as follows

$$C_A = \frac{31.62b_m}{(1-\omega)^2} \left(\frac{1}{q} - \frac{1}{b_f} \right) + \frac{73.632b_m t}{\left(\frac{b_f}{m_f} + \frac{b_m}{m_m} \right) (1-\omega)^2} \quad (31)$$

For the above equation, q and t must be chosen that satisfy the relation $t_D > [\omega(1-\omega)]/\lambda$.

1.4 Fracture Permeability Estimation

From Eqs. (12) and (17) and since C_A has been calculated, the fracture permeability is equal to

$$k_f = 70.6 \frac{b_f \mu B}{h(p_i - p_{wf})} \left[\ln \frac{2.2458A}{C_A r_w^2} \right] \quad (32)$$

1.5 Interporosity Flow Coefficient Estimation

The ability of the fluid to flow from the matrix into the fractures is governed by the parameter (λ) which is called the interporosity flow coefficient t . This parameter is defined as follow

$$\lambda = \alpha \left(\frac{k_m}{k_f} \right) r_w^2 \quad (33)$$

From Eqs. (15) and (17), interporosity flow parameter (λ) can be estimated

$$\lambda = 887.186 \frac{r_w^2 b_m \mu B}{A k_f h (p_i - p_{wf})} \quad (34)$$

1.6 Block Shape Factor Estimation

The parameter (α), block shape factor, can be determined by combining Eqs. (33) and (34)

$$\alpha = 887.186 \frac{b_m \mu B}{A k_m h (p_i - p_{wf})} \quad (35)$$

1.7 Average Reservoir Pressure Determination

It can be shown that during pseudo-steady state flow for a closed reservoir, the pressure behavior is given by (Tiab, 1995)

$$\overline{p_{wD}} = \overline{p_{wD}} + \frac{1}{2} \ln \left(\frac{2.2458A}{C_A r_w^2} \right) \quad (36)$$

and

$$\overline{p_{wD}} = \frac{kh}{141.2q\mu B} (\overline{p} - p_{wf}) \quad (37)$$

or if we have the initial reservoir pressure

$$\overline{p_{wD}} = \frac{kh}{141.2q\mu B} (p_i - \overline{p}) \quad (38)$$

combining Eq. (28) and Eq. (36)

$$\overline{p_{wD}} = \frac{2\pi t_D r_w^2}{A} + \frac{2\pi(1-\omega)^2 r_w^2}{\lambda A} \quad (39)$$

Using the above relation, the average reservoir pressure can be estimated, but it must be noticed that from the curve of q versus t , q and t must be chosen that satisfy $t_D > [\omega(1-\omega)]/\lambda$.

This point must be stated that r_w in all the above formulae is the effective wellbore radius and can be obtained by the equation $r_w = r_w' e^{-S}$, where r_w' is the actual wellbore radius, S is the skin factor and r_w is the effective wellbore radius. The skin is incorporated into the analysis by this equation and it must be noticed that a short build up test is better to be done to evaluate the skin factor and this build up test requirements for evaluating skin factor is the major limitation of this method.

1.8 Fracture Porosity and Width Determination

Once ω is calculated, the fracture porosity can be estimated if matrix porosity, ϕ_m , total matrix compressibility, c_{im} and total fracture compressibility, c_{if} are known as follows (Tiab et al., 2007)

$$\phi_f = (\phi c)_m \left(\frac{\omega}{1-\omega} \right) \times \frac{1}{c_{if}} \quad (40)$$

Fracture compressibility may be different from matrix compressibility by an order of magnitude. Naturally fractured reservoirs in Kirkuk Field (Iraq) and Asmari Field (Iran) have fracture compressibility ranging from 4×10^{-4} to 4×10^{-5} psi⁻¹. In Grozni Field (Russia) ranges from 7×10^{-4} to 7×10^{-5} . In all these reservoirs, c_{if} is 10 to 100 folds higher than c_{im} . Therefore, the practice of assuming $c_{if} = c_{im}$ is erroneous (Tiab et al., 2007).

The fracture compressibility can be estimated by using the following expression (Saidi, 1987)

$$c_{if} = \frac{1 - (k_f / k_{fi})^{1/3}}{\Delta p} \quad (41)$$

$$\Delta p = p_i - \bar{p} \tag{42}$$

where p_i : initial reservoir pressure; \bar{p} : current reservoir pressure; k_{fi} : fracture permeability obtained when the reservoir pressure was at or near initial condition p_i ; k_f : fracture permeability obtained at the current average reservoir pressure.

Matrix permeability is assumed to remain constant between the two tests (one test for obtaining k_f at the current reservoir pressure and another one for calculating k_{fi} at or near initial pressure, p_i). Note that the time between these two tests must be long enough for the fractures to deform significantly in order to determine an accurate value of c_{if} .

The fracture width or aperture may be estimated from (Bona et al., 2003)

$$w_f = \sqrt{\frac{k_f}{33\omega\phi_i}} \tag{43}$$

$$\phi_t = \phi_m + \phi_f \tag{44}$$

where fracture width is in microns, permeability, is in mD, porosity and storage capacity are fractions and dimensionless.

According to the above formulation and calculations, it may be concluded that if a rate transient test is conducted in a naturally fractured reservoir with known matrix storage capacity and skin factor, one can calculate all the important reservoir parameters accurately. The main application of this method is for naturally fractured reservoirs with unknown shapes. The performance of the presented method is evaluated in the following simulated and field examples.

1.8.1 Simulated example 1

Two rate transient tests were run in a cylindrical, naturally fractured reservoir using Saphir® software with different properties. In these tests, both fracture system and matrix+fracture system should exhibit pseudo steady state flow so that the proposed model could be applicable for estimating different reservoir properties since equations in the proposed model have been obtained for closed and bounded naturally fractured reservoirs. Rate versus time data for simulated example 1 is shown

in Fig. 1. Relevant information concerning fluid and reservoir properties is provided in Table 1.

1.8.2 Solution

Step 1: The log-log plot (diagnostic plot) of rate vs. time is provided in Fig. 1.

Step 2: The plots of flow rate versus time on semi-log graph for data points related to fracture system in PSS region and for data points related to fracture+matrix system in PSS region are given in Figs. 2 and 3, respectively.

Step 3: From Fig. 2, the values of the slope and intercept of the graph, m_f and b_f , are equal to -0.133 hr^{-1} and 837.15 STB/D , respectively.

Step 4: From Fig. 3, the values of the slope and intercept of the graph, m_m and b_m , are equal to $-1.27 \times 10^{-4} \text{ hr}^{-1}$ and 79.04 STB/D , respectively.

Step 5: Since $S = -4.09$, then $r_w = r'_w e^{-S} = 15 \text{ ft}$.

Step 6: From Eq. (22), storage capacity ratio is 0.01.

Step 7: From Eq. (27), reservoir drainage area calculated is $7\,198\,718.501 \text{ ft}^2$.

Step 8: Now, we need reservoir shape factor to calculate the other parameters. Using Eq. (31) and $q = 74 \text{ bbl/day}$ and $t = 48 \text{ hr}$ from the region of the depletion of total system (fracture+matrix), yields: $C_A = 30.96$.

Table 1 Fluid, well and reservoir data for simulated examples

Parameter	Simulated value	
	Example 1	Example 2
P_i (psi)	11 500	5 000
P_{wf} (psi)	5 000	3 500
B (RB/STB)	1.00	1.28
μ (cp)	1	0.487 5
Rw (ft)	0.25	0.3
Re (ft)	1 500	500
S	-4.09	0
H (ft)	480	200
ϕ	10%	10%
ω	0.01	0.01
λ	5×10^{-6}	1×10^{-8}
$(\phi c_t)_i$ (psi^{-1})	2.8×10^{-9}	1.6×10^{-7}

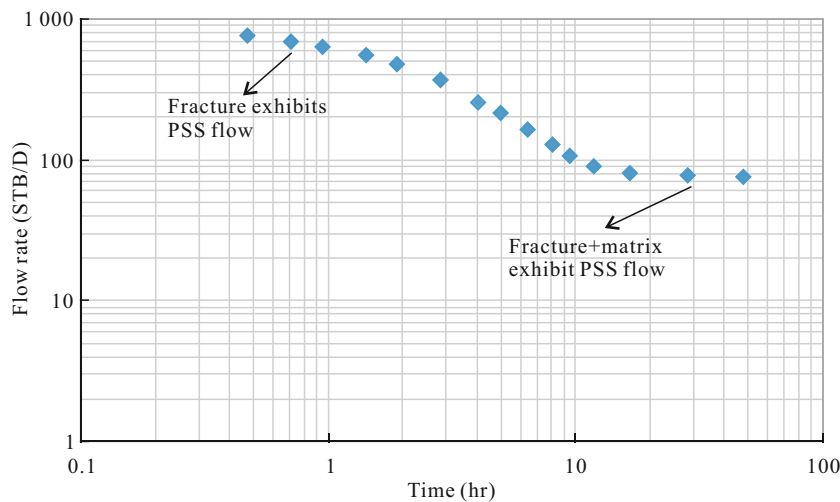


Figure 1. Log-log plot of rate versus time for simulated example 1.

Step 9: Fracture permeability is equal to 0.146 mD which is obtained from Eq. (32).

Step 10: Using Eq. (34), the interporosity flow parameter is 4.8×10^{-6} .

1.8.3 Simulated example 2

Estimate the parameters of a naturally fractured reservoir using the rate transient study as discussed in this manuscript for a simulated test in a homogeneous circular reservoir ($\omega=0.01$, $\lambda=1 \times 10^{-8}$) using the information given in Table 1.

1.8.4 Solution

Step 1: The log-log plot (diagnostic plot) of rate vs. time is provided in Fig. 4.

Step 2: The plots of flow rate versus time on semi-log graph for data points related to fracture system in PSS region and for data points related to fracture+matrix system in PSS region are given in Figs. 5 and 6, respectively.

Step 3: From Fig. 5, the values of the slope and intercept of the graph, m_f and b_f are equal to -0.013 hr^{-1} and 51.2 STB/D, respectively.

Step 4: From Fig. 6, the values of the slope and intercept of the graph, m_m and b_m , are equal to $-1.419 \times 10^{-5} \text{ hr}^{-1}$ and 4.2 STB/D, respectively.

Step 5: From Eq. (22), storage capacity ratio is 0.013.

Step 6: From Eq. (27), reservoir drainage area calculated is 784 352 ft^2 .

Step 7: Fracture permeability is equal to 0.100 4 md which is obtained from Eq. (32).

Step 8: Using Eq. (34), the interporosity flow parameter is 0.885×10^{-8} .

1.8.5 Field example

The following data were presented by Chen (1985) for a naturally fractured reservoir (Austin Chalk Formation) with a skin factor, S , of about -4. The data are illustrated in Table 2.

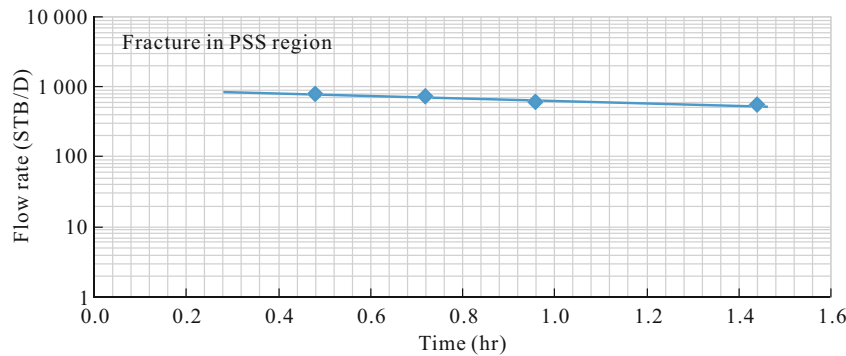


Figure 2. Log (q) versus time for fracture system in PSS region for simulated example 1.

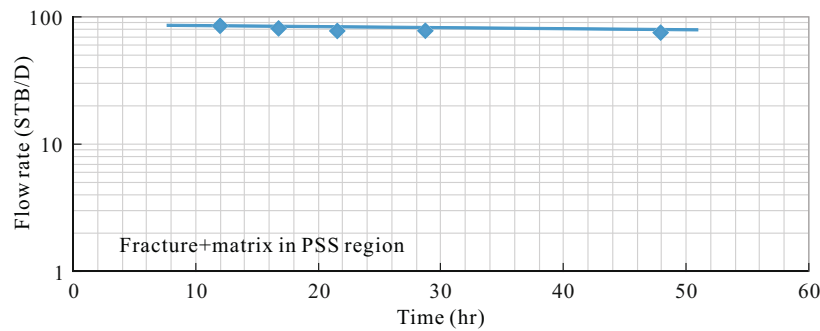


Figure 3. Log (q) versus time for total system (fracture+matrix) in PSS region for simulated example 1.

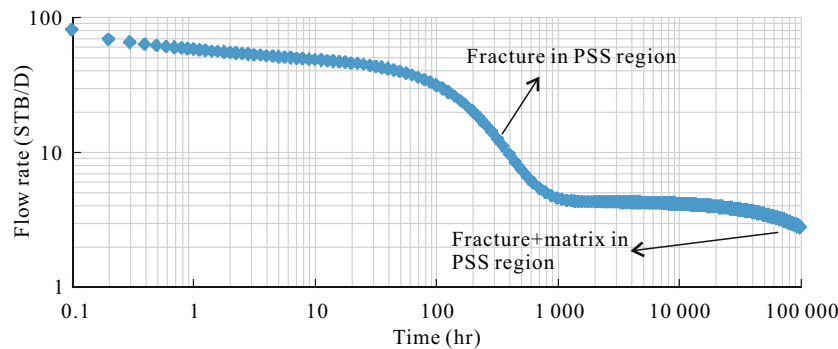


Figure 4. Log-log plot of rate versus time for simulated example 2.

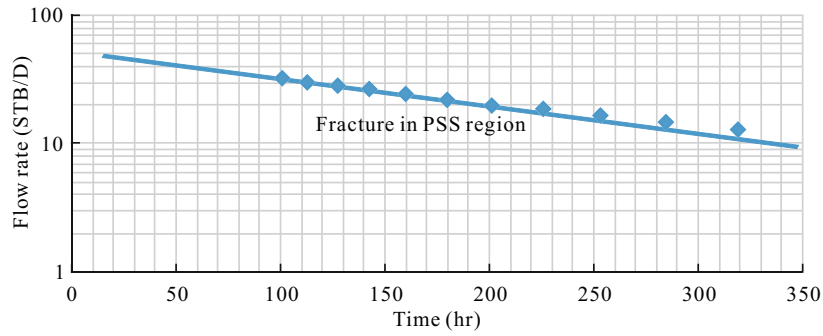


Figure 5. Log (q) versus time for fracture system in PSS region for simulated example 2.

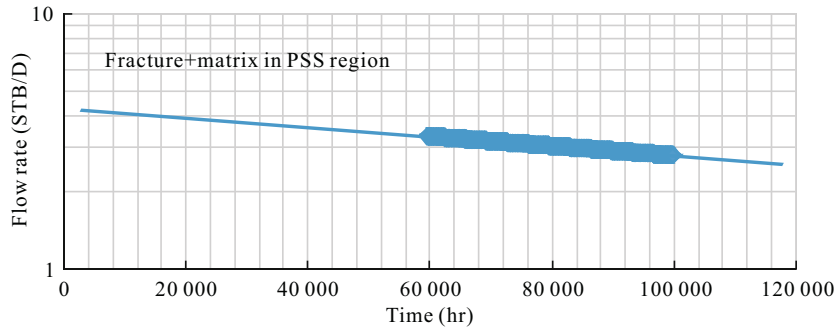


Figure 6. Log (q) versus time for total system (fracture+matrix) in PSS region for simulated example 2.

Table 2 Rate transient data for field example

Time (hr)	Q (bbl/day)	Time (hr)	Q (bbl/day)
1 306.4	238.86	10 787	50.8
1 941.4	248.3	11 468.5	46.1
2 783.1	234.3	12 207.2	46.1
3 459.3	189.37	12 995.3	42.7
4 241.1	153.06	13 676.8	38.7
4 968.4	119.02	14 362	38
5 756.4	110.1	15 149	34.5
6 327.1	89.04	15 886	33.2
7 220.7	82.4	16 518	32.5
7 953.2	72	17 304	28.4
8 630.4	59.3	18 044	27.6
9 420.2	57	18 724	25.81
9 998.9	54.9	19 353	23.4

$p_i=3\ 800\ \text{psi}$; $p_{wf}=0\ \text{psi}$; $r_w=0.25\ \text{ft}$; $S=-4.0$; $k_{fr}=0.82\ \text{md}$; $h=40\ \text{ft}$; $\phi_m=10\%$; $\mu=0.26\ \text{cp}$; $C_m=3.041\times 10^6\ \text{psi}^{-1}$; $B=1.58\ \text{RB/STB}$; $k_m=0.28\ \text{md}$.

1.8.6 Solution

Step 1: The semi-log plot of flow rate vs. time is provided in Fig. 7. Different regions are illustrated in this figure.

Step 2: From Fig. 7, the values of the slope and intercept of the graph, m_f and b_f , are equal to $-1.368\times 10^{-4}\ \text{hr}^{-1}$ and 578.8 STB/D, respectively.

Step 3: From Fig. 7, the values of the slope and intercept of the graph, m_m and b_m , are equal to $-3.701\times 10^{-5}\ \text{hr}^{-1}$ and 126.7 STB/D, respectively.

Step 4: Since $S=-4$, then $r_w = r'_w e^{-S} = 13.6\ \text{ft}$.

Step 5: From Eq. (22), storage capacity ratio is 0.552 7.

Step 6: Using Eq. (24) and the obtained ω , fracture storage capacity is $3.757\times 10^{-7}\ \text{psi}^{-1}$. Then, total storage capacity would

be $6.8\times 10^{-7}\ \text{psi}^{-1}$.

Step 7: From Eq. (27), reservoir drainage area calculated is $1\ 751\ 764.706\ \text{ft}^2$.

Step 8: Now, we need reservoir shape factor to calculate the other parameters. Using Eq. (31) and $q=23.4\ \text{bbl/day}$ and $t=19\ 353\ \text{hr}$ from the region of the depletion of total system (fracture+matrix), yields: $C_A=30$.

Step 9: Fracture permeability is equal to 0.72 mD which is obtained from Eq. (32).

Step 10: Using Eq. (34), the interporosity flow parameter is 4.45×10^{-5} .

Step 11: From Eq. (35), block shape factor is $6.194\times 10^{-7}\ \text{ft}^2$.

For this example, type curve matching approach is also performed. This method is the conventional method that is used for rate transient well test analysis for naturally fractured reservoirs. Results are indicated in Table 3. For applying type curve matching, ω and λ must be estimated previously by another method like build-up analysis. Chen (1985) calculated these parameters from the data of build-up test (Table 3).

2 CONCLUSIONS

In this study, a method based on rate transient decline curve analysis was developed in order to estimate different properties of naturally fractured reservoirs. For a naturally fractured reservoir, when both fracture system and total (fracture+matrix) system exhibit pseudo-steady state flow regime, properties for instance storage capacity ratio, fracture and total storage capacity, reservoir drainage area, reservoir shape factor, fracture permeability, interporosity flow coefficient, block shape factor and the other parameters can be estimated by using the governing equations of these two regions. These equations show that when $\ln(\text{flow rate})$ is plotted versus time, two straight lines, related to the two regions, are obtained and

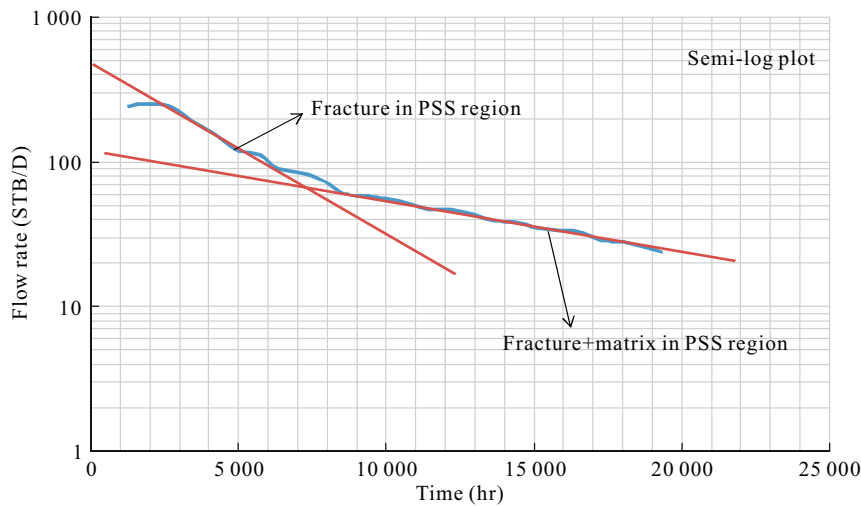


Figure 7. Log (q) versus time for field example.

Table 3 Comparison between the results obtained by two different methods for field example

Variable	Type curve method	This work	Error (%)
ω	0.552 7 (estimated by Chen, 1985)	0.552 7	0
Drainage area (ft ²)	1 742 258.45	1 751 764.71	0.54
$(\phi c_v)_f$ (psi ⁻¹)	3.757×10^{-7}	3.757×10^{-7}	0
$(\phi c_v)_i$ (psi ⁻¹)	6.8×10^{-7}	6.8×10^{-7}	0
λ	4.50×10^{-5} (estimated by Chen, 1985)	4.45×10^{-5}	-1.1
k_f (mD)	0.64	0.72	12.1
C_A	31.62	30	-5.12
α (ft ⁻²)	5.6×10^{-7}	6.194×10^{-7}	10.6

their slopes and intercepts can be used for approximating different properties. In the proposed approach, no chart is used and since pseudo-steady state flow regime is implemented, the influence of wellbore storage on the estimation of the parameters is negligible. One of the most important advantages of this method is that nearly all the parameters could be estimated directly, while in type curve matching method, ω and λ must be determined using build-up analysis. Therefore, using the proposed approach would save time during reservoir analyses. Different simulated and field examples were used for testing the proposed method. Results demonstrated that the obtained parameters by the proposed procedure compared quite well with the results of conventional method such as type curve matching approach.

3 NOMENCLATURE

- A : Drainage area, ft².
- B : Oil volumetric factor, RB/STB.
- b : Intercept of $\ln(q)$ versus time plot, hr⁻¹.
- C : System compressibility, psi⁻¹.
- C_A : Reservoir shape factor, dimensionless.
- h : Net pay thickness, ft.
- I_0 : Modified Bessel Function second kind order zero.
- I_1 : Modified Bessel Function second kind order one.
- K_0 : Modified Bessel Function first kind order zero.
- K_1 : Modified Bessel Function first kind order one.
- k : Permeability, mD.
- m : Slope of $\ln(q)$ versus time plot, hr⁻¹.

- p : Pressure, psi.
- \bar{p} : Current reservoir pressure, psi.
- q : Oil flow rate, STB/D.
- r : Radius, ft.
- r_D : r/r_w , dimensionless.
- r_w : Effective well bore radius, ft.
- s : Laplace variable.
- S : Skin factor, dimensionless.
- t : Time, hr.
- w : Width, microns.

Greek

- ϕ : Porosity, dimensionless.
- α : Block shape factor, $1/L^2$.
- λ : Interporosity flow parameter, dimensionless.
- μ : Viscosity, cp.
- ω : Storage capacity ratio, dimensionless.

Subscripts

- D : Dimensionless.
- f : Fracture.
- h : Homogeneous.
- I : Initial.
- m : Matrix.
- t : Total.
- wf : Well bore flowing.

APPENDIX A

Derivation of Dimensionless Slope and Dimensionless Intercept Parameters

The following dimensionless parameters for flow rate and time are known

$$q_D = 141.2 \frac{q\mu B}{k_f h(p_i - p_{wf})} \quad (\text{A-1})$$

$$t_D = 2.637 \times 10^{-4} \frac{k_f t}{[(\phi c_t)_f + (\phi c_t)_m] \mu r_w^2} \quad (\text{A-2})$$

Since the intercept of the graph of $\ln(\text{flow rate})$ versus time shows the flow rate, the dimensionless intercept parameter can be defined as same as dimensionless flow rate

$$b_D = 141.2 \frac{b\mu B}{k_f h(p_i - p_{wf})} \quad (\text{A-3})$$

The slope of the plot can be defined as follow

$$m = \frac{\log(q_2 / q_1)}{t_2 - t_1} \quad (\text{A-4})$$

In this method we used the plot of $\ln(\text{rate})$ versus time, so the dimensionless slope is

$$m_D = \frac{\ln(q_{D2} / q_{D1})}{t_{D2} - t_{D1}} = \frac{\log(q_{D2} / q_{D1})}{0.434(t_{D2} - t_{D1})} \quad (\text{A-5})$$

Substituting (A-1) and (A-2) into (A-5) yields

$$m_D = 873.3m \frac{[(\phi c_t)_f + (\phi c_t)_m] \mu r_w^2}{k_f} \quad (\text{A-6})$$

ACKNOWLEDGMENT

Thanks go to the reviewers and the editors for their helpful suggestions. The final publication is available at Springer via <https://doi.org/10.1007/s12583-017-0776-y>.

REFERENCES CITED

- Abbasi, M., Hossieni, M., Izadmehr, M., et al., 2016. Tracer Transport in Naturally Fractured Reservoirs: Analytical Solutions for a System of Parallel Fractures. *International Journal of Heat and Mass Transfer*, 103(2016): 627–634. doi:10.1016/j.ijheatmasstransfer.2016.07.078
- Abramowitz, M., Stegun, I. A., 1972. Handbook of Mathematical Functions. Dover Publications Inc., New York
- Bona, N., Radaelli, F., Ortenzi, A., et al., 2003. Integrated Core Analysis for Fractured Reservoirs: Quantification of the Storage and Flow Capacity of Matrix, Vugs, and Fractures. *SPE Reservoir Evaluation & Engineering*, 6(4): 226–233. doi:10.2118/85636-pa
- Bourbiaux, B., Granet, S., Landereau, P., et al., 1999. Scaling up Matrix-Fracture Transfers in Dual-Porosity Models: Theory and Application. Paper SPE-56557-MS Presented at the SPE Annual Technical Conference and Exhibition, Houston. doi:10.2118/56557-MS.
- Chen, H. Y., 1985. A Reservoir Engineer Characterization of the Austin Chalk Trend: [Dissertation]. Texas A&M University, Texas
- Da Prat, G., Cinco-Ley, H., Ramey, H. Jr., 1981. Decline Curve Analysis Using Type Curves for Two-Porosity Systems. *Society of Petroleum Engineers Journal*, 21(3): 354–362. doi:10.2118/9292-pa
- de Swaan, A., 1990. Influence of Shape and Skin of Matrix-Rock Blocks on Pressure Transients in Fractured Reservoirs. *SPE Formation Evaluation*, 5(4): 344–352. doi:10.2118/15637-pa
- Duguid, J. O., Lee, P. C. Y., 1977. Flow in Fractured Porous Media. *Water Resources Research*, 13(3): 558–566. doi:10.1029/wr013i003p00558
- Gang, T., Kelkar, M. G., 2006. Efficient History Matching in Naturally Fractured Reservoirs. Paper SPE-99578-MS Presented at the SPE/DOE Symposium on Improved Oil Recovery, Tulsa, Oklahoma. doi:10.2118/99578-MS.
- Gilman, J. R., 1986. An Efficient Finite-Difference Method for Simulating Phase Segregation in the Matrix Blocks in Double-Porosity Reservoirs. *SPE Reservoir Engineering*, 1(4): 403–413. doi:10.2118/12271-pa
- Gutmanis, J., 2009. Basement Reservoirs—A Review of Their Geological and Production Characteristics. Paper IPTC-13156-MS Presented in International Petroleum Technology Conference, Doha, Qatar. doi:10.2523/IPTC-13156-MS
- Igbokoyi, A. O., Tiab, D., 2006. Estimation of Average Reservoir Pressure and Drainage Area in Naturally Fractured Reservoirs—Tiab's Direct Synthesis. SPE-104060-MS Presented at the First International Oil Conference and Exhibition in Mexico, Cancun. 1–13. doi:10.2118/104060-MS
- Landereau, P., Noetinger, B., Quintard, M., 2001. Quasi-Steady Two-Equation Models for Diffusive Transport in Fractured Porous Media: Large-Scale Properties for Densely Fractured Systems. *Advances in Water Resources*, 24(8): 863–876. doi:10.1016/s0309-1708(01)00015-x
- Mavor, M. J., Cinco-Ley, H., 1979. Transient Pressure Behavior of Naturally Fractured Reservoirs. Paper SPE-7977-MS Presented at the SPE California Regional Meeting, Houston. 18–20. doi:10.2118/7977-MS
- Noetinger, B., Estebenet, T., 2000. Up-Scaling of Double Porosity Fractured Media Using Continuous-Time Random Walks Methods. *Transport in Porous Media*, 39: 315–337. doi:10.1023/A:1006639025910
- Pruess, K., 1985. A Practical Method for Modeling Fluid and Heat Flow in Fractured Porous Media. *Society of Petroleum Engineers Journal*, 25(1): 14–26. doi:10.2118/10509-pa
- Saidi, M. A., 1987. Reservoir Engineering of Fractured Reservoirs. Total Edition Press, Paris. 289
- Stehfest, H., 1970. Algorithm 368: Numerical Inversion of Laplace Transforms [D5]. *Communications of the ACM*, 13(1): 47–49. doi:10.1145/361953.361969
- Tiab, D., 1994. Analysis of Pressure Derivative without Type-Curve Matching: Vertically Fractured Wells in Closed System. *Journal of Petroleum Science and Engineering*, 11: 323–333
- Tiab, D., 1995. Analysis of Pressure and Pressure Derivative without Type-Curve Matching, Skin and Wellbore Storage. *Journal of Petroleum Science and Engineering*, 12: 171–181
- Tiab, D., Igbokoyi, A., Restrepo, D., 2007. Fracture Porosity from Pressure Transient Data. International Petroleum Conference, Bratislava. 8. doi:10.2523/IPTC-11164-MS.
- van Everdingen, A. F., Hurst, W., 1949. The Application of the Laplace Transformation to Flow Problems in Reservoirs. *Journal of Petroleum Technology*, 1(12): 305–324. doi:10.2118/949305-g
- Warren, J. E., Root, P. J., 1963. The Behavior of Naturally Fractured Reservoirs. *Society of Petroleum Engineers Journal*, 3(3): 245–255. doi:10.2118/426-pa